Supplementary Materials

Supplementary Methods

Sample collection

A field investigation of *L. taliangensis* was conducted in the breeding seasons from 2016 to 2019, and 426 tissue samples were collected from 16 sites throughout the southeastern Hengduan Mountains Region (HMR) in China (Figure 1; Supplementary Table S1). Samples were preserved in 95% absolute ethanol and stored at −20 °C. The tissue samples included tail tips of larvae and toes of adults. All individuals were released back to their place of capture after wound disinfection.

DNA extraction, amplification, and sequencing

Three mitochondrial DNA (mtDNA) fragments were extracted from the 426 tissue samples using a TIANGEN Animal Genomic DNA Kit (TIANGEN Biotech Co., Ltd., Beijing, China) following the manufacturer's protocols. Polymerase chain reaction (PCR) was performed in a 25 µl volume, containing 2 µl of template DNA solution, 12.5 µl of 2×Taq Master Mix (Vazyme Biotech Co., Ltd., Nanjing, China), 1 µl of each primer, and 8.5 µl of ddH_2O. The following PCR cycling conditions were applied: initial denaturation at 94 °C for 4 min, 35 cycles at 94 °C for 40 s, annealing (annealing temperature is given in Supplementary Table S2) for 40 s, extension at 72 °C for 70 s, and final extension at 72 °C for 8 min. Identification and visualization of amplification product lengths were performed using 1.2% agarose gel electrophoresis on an ABI 3730xl DNA sequencer (Sangon Biotech Co., Ltd., Shanghai, China).

Microsatellite genotyping

Eleven highly polymorphic microsatellite loci were used as gene markers (Chen et al., 2019; Shu, 2020). The 5' ends of each forward primer pair were labeled with one of three fluorescent dyes, i.e., FAM, HEX, or TAMRA. The PCR amplification system and conditions followed those of Chen et al. (2019) and Shu (2020). The PCR products with different dye analyses were visualized on an ABI 3730xl DNA sequencer (Sangon Biotech Co., Ltd., Shanghai, China) and genotyped using GeneMarker HID v1.95 (SoftGenetics, LLC, State College, PA, USA).

Divergence date estimation

PartitionFinder v2.1.1 (Lanfear et al., 2017) was run to determine gene partition strategies and the optimal nucleotide substitution before BEAST analysis. Markov chain Monte Carlo (MCMC) analyses were performed assuming a "unlinked uncorrected lognormal relaxed clock" under the Yule speciation model. Bayesian MCMC chains were run for 10 million generations, with sampling every 1 000 generations and the first 10% of generations discarded as burn-in. Effective sampling size convergence and stationarity (ESS) was estimated by checking the logfile in TRACER v1.7 (Rambaut et al., 2018). A maximum clade credibility (MCC) tree was

calculated using TreeAnnotator v1.8.2 (Drummond & Rambaut, 2007).

Demographic estimation (Bayesian skyline plot construction)

A strict molecular clock, the mean rate (0.475% site-1 million-1 years-1) of which was evaluated from the second step of divergence date estimation analysis, and the piecewise-constant model were chosen as the tree prior skyline model. Runs of 10 million generations were performed, with samples taken every 1 000 iterations and the first 10% discarded as burn-in.

Migration pattern analysis

Three demographic models were estimated: (1) only from the West cluster (XXL-GG) to the East cluster (LS); (2) only from the East cluster (LS) to the West cluster (XXL-GG); and (3) two-way migration between the West cluster (XXL-GG) and East cluster (LS). These analyses were based on the grouping of microsatellite genotypes from all samples into two clusters (results of population structure in Figure 1). For analysis, 20 independent replicates with four heated chains under the following temperatures were applied: 1.0, 1.5, 3.0, and 100 000; each replicate had 8 000 000 MCMC steps, with a burn-in of 80 000 and sampling every 100 iterations. To identify the optimal model, the ln Bayes factors (BF) were calculated based on the differences between log marginal likelihood values (Beerli & Palczewski, 2010).

Ecological niche modeling

Variables included the Last Interglacial (LIG, 120 ka) and Last Glacial Maximum (LGM, 21 ka) with three general circulation models (GCMs) (CCSM4, MIROC-ESM, and MPI-ESM-P), mid-Holocene (MH, 6 ka) with four GCMs (CCSM4, MIROC-ESM, MPI-ESM-P, and BCC-CSM1-1), and the present. To maintain consistent climate raster resolution, the resolution of the LGM rasters was increased from 2.5 min to 30 arc-seconds by the "resample" method in ArcGIS v10.3.

Before constructing the ENM, bioclimatic rasters were clipped into the study area from 25–31°N to 100–105°E, and rasters were converted to the ASCII format for MaxEnt analysis. To prevent over-fitting, "band collection statistic" of the spatial analysis tool was used to calculate the correlation coefficients between different bioclimatic rasters in ArcGIS v10.3. Variables included in the ENM were not highly correlated with each other (correlation coefficient<0.8). The following five bioclimatic predictors were retained: isothermality (Bio03), minimum temperature of coldest month (Bio06), annual temperature range (Bio07), annual precipitation (Bio12), and precipitation of driest month (Bio14).

The predictive effectiveness of MaxEnt can be affected by both "feature types" and "regularization constants", especially for small sample sizes. The following different parameters were set: "L, LQ, H, LQH, LQP, and LQPH" for "feature types" and 0.5–4 for "regularization constants"; then, the optimal parameters were selected based on the minimum value of the corrected Akaike information criterion (AICc) calculated by ENMTOOLS v1.4.3 (Warren et al., 2010).

ENM was conducted in MaxEnt v3.4.1. Here, 10 000 background points were set,

and the logistic output format and each model were run with 10 cross-validation replicates. The averages of projections of 10 iterations were used as the prediction results of each time period. Projections were then averaged across the three GCMs for LGM and four GCMs for MH to arrive at the final distribution prediction for these two periods.

Isolation-by-resistance (IBR) as an alternative to IBD

Euclidean geographical distance was once commonly used as a geographic factor to explain population differentiation (IBD; Wright, 1943); however, interpopulation migration is not straightforward, and Euclidean geographical distance cannot completely reflect the impact of landscape heterogeneity. Resistance distance, a geographic distance metric based on circuit theory, is a reliable and stable predictor of genetic divergence compared to traditional distance measures (e.g., Euclidean geographical distance) (Emel et al., 2021; McRae, 2006; McRae et al., 2008; Myers et al., 2019; Vasconcellos et al., 2019; Wang, 2013). Here, instead of Euclidean geographical distances, resistance distances can reflect topographic complexity and population connectivity as a new geographic distance metric.

Resistance surface construction

Twenty-three environmental rasters (including 19 bioclimatic variables, altitude, normalized difference vegetation index (NDVI) (1998–2018 average), Global Human Influence Index (HII), and river) were used to develop an ENM for the 26–31°N to 101–105°E region.

Bioclimatic variables and altitudinal data were downloaded from the WorldClim website (https://www.worldclim.org); NDVI (1998–2018) and river (.shp format) data were obtained from the Resource and Environment Science and Data Center (http://www.resdc.cn). Distance analysis (Euclidean distance) of river layers was conducted in ArcGIS v10.3 to construct a new river raster for MaxEnt analysis; HII was derived from EARTHDATA (https://sedac.ciesin.columbia.edu). All variable rasters had a resolution of 30 s.

Before construction of the ENM, the correlation coefficients between different rasters were calculated in ArcGIS v10.3, and variables with high correlation (correlation coefficient≥0.8) were removed. Finally, the following nine environmental predictors were selected: temperature seasonality (Bio04), temperature annual range (Bio07), annual precipitation (Bio12), precipitation of driest month (Bio14), precipitation seasonality (Bio15), altitude, NDVI, HII, and river. Furthermore, model parameter filtering was performed using ENMTOOLS v1.4.3 (Warren et al., 2010).

A grid cell of an ENM raster with a higher suitability score means a lower friction value; therefore, here, the ENM grids were inverted to create a resistance surface to calculate the resistance distance in Circuitscape v4.0 (McRae, 2006; McRae et al., 2016).

Environmental dissimilarity matrix calculation

Nineteen bioclimate variables (https://www.worldclim.org) and NDVI

(https://www.resdc.cn) with 30 arc-second resolutions were extracted from each site in ArcGIS, and two principal components (PCs) were obtained (PC1: 58.98% and PC2: 29.23%). The two sets of environmental dissimilarity matrices, used for isolation-by-environment (IBE) analysis (Wang & Bradburd, 2014), were calculated separately by the two PCs using the "*dist*" function in R v3.6.1.

Supplementary Tables

Supplementary Table S1 Sampling information of *L. taliangensis* in southeastern Hengduan Mountains Region

Mountains		Location	Population code	Sample size (N)		Altitude (m)	Longitude (°E)	Latitude (°N)
				Mt DNA (407)	SSR (426)			
Xiaoxiangling (XXL)		Pusagang, Mianning	PSG	28	28	2518	102.3081	28.8991
		Zhuma, Shimian	ZUM	24	26	1688	102.4308	29.1356
		Zima, Shimian	ZM	20	20	1984	102.2736	28.9809
		Yeniuhe, Shimian	YNH	16	17	2201	102.2809	29.0147
		Jinghuahu, Shimian	JHH	22	22	2607	102.2858	28.9738
		Gongyihai, Shimian	GYH	46	46	2019	102.3932	29.0205
Gonggar (GG)		Xinmin, Shimian	XM	36	42	2410	102.1889	29.3715
Liangshan (LS)	Xiaoliangshan (XLS)	Ganluo	GL	23	23	3022	102.8545	28.9663
		Chuhongjue, Meigu	CHJ	29	30	2837	103.1300	28.6448
		Longwo, Meigu	LW	39	41	2172	103.2017	28.7188
		Bingtu, Meigu	BT	27	28	2319	103.0488	28.5686
		Shengliping, E'bian	SLP	22	22	2279	103.0502	28.7367
		Sanhekou, Mabian	SHK	35	40	1700	103.3246	28.8811
	Daliangshan (DLS)	Qiliba, Zhaojue	QLB	22	23	3140	102.5240	27.8734
		Wuke, Butuo	WK	12	12	3214	102.7444	27.5974
		Yuexi	YX	6	6	2206	102.5774	28.4582

Supplementary Table S2 Amplification primer pairs for three mitochondrial gene markers

Gene marker	Primer Pairs	Primer sequence	Annealing temperature (℃)	Amplified fragment length (bp)	References
cyt *b*	MVZ-F	5'-GAACTAATGGCCCACAC(AA/TT)TACGNAA-3'	49	823	Moritz et al., 1992
	MVZ-R	5'-AAATAGGAA(A/G)TATCA(T/C)TCTGGTTT(A/G)AT-3'			
	2cyt *b*-F	5'-ACCAAGACCTCTGACCTG-3'	50.2	980	This study
	2cyt *b*-R	5'-GTATGTAATAATGGGAAG-3'			
	3cyt *b*-F	5'-AACCCACCCACTAATAAA-3'	52	832	This study
	3cyt *b*-R	5'-ATAGAGCGAAGGATTGCGTAAGC-3'			
ND2	Pmet	5'-AAGCTTTTGGGCCCATACC-3'	53	1100	Wang et al., 2009
	Ptrp	5'-TRCTTABGGCTTTGAAGG-3'			
	ND2-F	5'-TACTAATGAACCCACACG-3'	50.2	1054	This study
	ND2-R	5'-AGTCTTTAGTTTAGTATT-3'			
COI	*COI*-F	5'-TATATGCTAGACATCACAGG-3'	60.7	1716	This study
	COI-R	5'-TTGAAGAAGGTGGTAGATTG-3'			
	3*COI*-F	5'-CACAGGGCTTGGTAAA-3'	54.4	1800	This study
	3*COI*-R	5'-GATGCGGCGTCTTGAAAACC-3'			

Supplementary Table S3 GenBank number of outgroup species

Outgroup species name	GenBank number
Tylototriton kweichowensis	NC_029231
Tylototriton shanorum	KU255459
Tylototriton verrucosus	AB689009
Tylototriton yangi	KU297946
Tylototriton shanjing	KR154461
Tylototriton ziegleri	KY398015
Tylototriton asperrimus	EU880340
Tylototriton wenxianensis	NC_027507

Supplementary Table S4 GenBank numbers of four calibration points (C1–C4) and of other Salamandridae species used in first step of molecular dating analysis

	Species	GenBank number
C1	*Pleurodeles poireti*	EU880329
(Estes, 1981	*Pleurodeles waltl*	EU880330
Herre, 1935	*Echinotriton chinhaiensis*	EU880315
Milner, 2000)	*Echinotriton andersoni*	EU880314
C2	*Notophthalmus viridescens*	EU880323
(Estes, 1981)	*Notophthalmus meridionalis*	EU880322
	Taricha rivularis	EU880334
	Taricha granulosa	EU880333
C3	*Triturus marmoratus*	EU880337
(Böhme, 2003)	*Triturus cristatus*	EU880336
C4	*Cynops orientalis*	EU880311
(Estes, 1981)	*Cynops pyrrhogaster*	EU880313
	Paramesotriton deloustali	EU880327
	Laotriton laoensis (*Paramesotriton laoensis*)	EU880328
	Pachytriton labiatus	EU880325
Others	*Euproctus platycephalus*	EU880317
	Ichthyosaura alpestris (*Mesotriton alpestris*)	EU880335
	Calotriton asper	EU880307
	Neurergus kaiseri	EU880320
	Salamandrina terdigitata	EU880332
	Chioglossa lusitanica	EU880308
	Lyciasalamandra atifi	AF154053
	Salamandra salamandra	EU880331

Supplementary Table S5 Haplotypes of concatenated genes and sequence names

Hap	Frequency	Sequences name
Hap_1	33	BT01-02,04-28
		CHJ01,06,08,10,19,22
Hap_2	1	CHJ02
Hap_3	9	CHJ03,07,14-15,25,27,30
		LW04,21
Hap_4	1	CHJ04
Hap_5	7	CHJ05,13,17-18,21,24,28
Hap_6	1	CHJ09
Hap_7	3	CHJ11-12,26
Hap_8	1	CHJ16
Hap_9	1	CHJ20
Hap_10	1	CHJ29
Hap_11	1	GL01
Hap_12	9	GL02-04,06,09,12,14,17,23
Hap_13	1	GL05
Hap_14	3	GL07,11,18
Hap_15	3	GL08,10,19
Hap_16	4	GL13,16,20,22
Hap_17	1	GL15
Hap_18	1	GL21
Hap_19	38	GYH01-04,07,09-20,23,26-32,34-36,38-46
		JHH18
Hap_20	5	GYH05,08,21,22,24
Hap_21	68	GYH06,33,37
		JHH02-03,07,09-11,14,19,22
		PSG01-09,11-19,21-25,27-28
		YNH01-04,06-11,13-16
		ZM01-03,05-09,11-19
Hap_22	1	GYH25
Hap_23	6	JHH01,12-13,16,20
		ZM20
Hap_24	10	JHH04-06,08,15,17,21
		PSG20
		ZM04,10
Hap_25	3	LW01,14,26
Hap_26	46	LW02,06-07,10-11,13,15,17,19-20,23,32-35,37-38
		SHK01-07,09,13-15,18-20,22-26,29-30,32-33,35-40
Hap_27	3	LW03,16,29
Hap_28	15	LW05,08,12,18,22,24-25,27-28,30-31,40
		SLP04,10,20
Hap_29	1	LW36

Hap_30	1	LW39
Hap_31	1	PSG10
Hap_32	1	PSG26
Hap_33	3	QLB01,31,33
Hap_34	7	QLB02,06-07,26-27,32,34
Hap_35	6	QLB03,05,09,14,16,29
Hap_36	5	QLB08,23-25,28
Hap_37	1	QLB30
Hap_38	3	SHK08,11,31
Hap_39	1	SHK10
Hap_40	1	SHK17
Hap_41	1	SHK21
Hap_42	15	SLP01-03,09,11-19,21-22
Hap_43	2	SLP05-06
Hap_44	2	SLP07-08
Hap_45	6	WK01,03,06,08-10
Hap_46	4	WK02,04-05,07
Hap_47	2	WK11-12
Hap_48	8	XM02,22,24,27,40,45-47
Hap_49	8	XM03,11-12,18,29,34-35,42
Hap_50	13	XM08-09,20-21,26,30,32,36-39,43-44
Hap_51	1	XM10
Hap_52	1	XM14
Hap_53	1	XM15
Hap_54	1	XM19
Hap_55	1	XM28
Hap_56	2	XM33,41
Hap_57	2	YNH05,12
Hap_58	3	ZUM01,07,22
Hap_59	10	ZUM02-03,06,08,13-14,16-17,21,23
Hap_60	5	ZUM04-05,09-10,24
Hap_61	5	ZUM12,15,18-19,25
Hap_62	1	ZUM20
Hap_63	1	YX01
Hap_64	1	YX02
Hap_65	1	YX03
Hap_66	2	YX04-05
Hap_67	1	YX06

Supplementary Table S6 Results of genetic diversity for each population based on mitochondrial genes

Populations	H	Hd	π
PSG	4	0.206 ± 0.100	0.00031 ± 0.00024
JHH	4	0.710 ± 0.049	0.00161 ± 0.00026
XM	9	0.786 ± 0.042	0.00050 ± 0.00011
ZUM	5	0.754 ± 0.056	0.00340 ± 0.00086
GYH	4	0.344 ± 0.085	0.00011 ± 0.00003
ZM	3	0.279 ± 0.123	0.00075 ± 0.00039
YNH	2	0.233 ± 0.126	0.00014 ± 0.00008
LW	7	0.718 ± 0.051	0.00062 ± 0.00009
CHJ	10	0.852 ± 0.036	0.00836 ± 0.00040
BT	1	-	-
QLB	5	0.788 ± 0.042	0.00109 ± 0.00011
WK	3	0.667 ± 0.091	0.00056 ± 0.00008
SHK	5	0.313 ± 0.099	0.00036 ± 0.00022
SLP	4	0.524 ± 0.116	0.00400 ± 0.00124
GL	6	0.810 ± 0.062	0.00527 ± 0.00031
YX	5	0.933 ± 0.122	0.00051 ± 0.00013

Notes: H, number of haplotypes; Hd, haplotype diversity; π, nucleotide diversity

Supplementary Table S7 Results of genetic diversity, neutrality test, and mismatch distribution analysis for all populations and two main clades of *L. taliangensis*

Populations	**N**	**H**	***π***	**Hd**	**Tajima's D (*P*)**	**Fu's F_S (*P*)**	**SSD (*P*)**	**H*rag* (*P*)**
All	407	67	0.00860 ± 0.00015	0.937 ± 0.006	0.54189 (0.769)	2.69639 (0.732)	0.01616 (0.000)**	0.01014 (0.000)**
South clade	77	18	0.00153 ± 0.00008	0.795 ± 0.043	-0.17659 (0.470)	-1.67923 (0.300)	0.03318 (0.070)	0.04707 (0.160)
North clade	330	49	0.00702 ± 0.00016	0.915 ± 0.008	0.28641 (0.708)	4.59049 (0.812)	0.05236 (0.000)**	0.01630 (0.040)*

Notes: N, sample size; H, number of haplotypes; π, nucleotide diversity; Hd, haplotype diversity; SSD, sum of square differences; H*rag*, Harpending's raggedness index

Statistical significance (*P*): *0.01 < *P* < 0.05; **0.001 < *P* < 0.01; *** *P*< 0.001

Supplementary Table S8 Genetic diversity and fixation index for each population and two main genetic clusters of *L. taliangensis* based on microsatellite data

Populations	N	TA	Ar	pAr	Ne	Ho (SE)	uHe (SE)	F_{IS}
XM	42	43	2.716	0.591	2.120	0.383 (0.071)	0.436 (0.076)	0.154
ZUM	26	49	3.464	0.298	2.921	0.531 (0.086)	0.567 (0.078)	0.039
GYH	46	43	2.751	0.085	2.196	0.417 (0.090)	0.420 (0.085)	-0.011
YNH	17	30	2.387	0.006	1.848	0.348 (0.068)	0.385 (0.075)	0.033
JHH	22	33	2.449	0.028	1.856	0.393 (0.074)	0.404 (0.069)	0.023
ZM	20	28	2.182	0.037	1.764	0.373 (0.074)	0.386 (0.067)	0.026
PSG	28	32	2.316	0.095	1.826	0.370 (0.073)	0.382 (0.072)	0.004
GL	23	68	4.389	0.573	3.815	0.664 (0.055)	0.695 (0.045)	0.032
SHK	40	48	3.370	0.185	2.921	0.559 (0.075)	0.579 (0.071)	0.030
SLP	22	43	3.136	0.154	2.700	0.545 (0.085)	0.544 (0.072)	0.030
LW	41	52	3.320	0.049	2.624	0.608 (0.051)	0.575 (0.046)	-0.074
CHJ	30	60	3.826	0.125	3.159	0.591 (0.048)	0.641 (0.046)	0.066
BT	28	32	2.193	0.011	1.763	0.360 (0.086)	0.357 (0.074)	0.012
YX	6	45	4.091	0.547	3.129	0.576 (0.088)	0.640 (0.063)	0.058
QLB	23	55	3.908	0.250	3.295	0.644 (0.035)	0.643 (0.049)	-0.044
WK	12	36	2.754	0.117	2.053	0.447 (0.082)	0.448 (0.069)	-0.021
West cluster	201	82	7.040	1.944	2.790	0.405 (0.058)	0.567 (0.063)	0.310
East cluster	225	119	9.917	4.820	4.653	0.560 (0.038)	0.737 (0.038)	0.241

Note: N, sample size of each population; TA, total number of alleles; Ar, allele richness; pAr, private allele richness, standardized for sample size; Ne, number of effective alleles; Ho, observed heterozygosity; uHe, unbiased expected heterozygosity; SE, standard error; F_{IS}, fixation index/inbreeding coefficient.

Supplementary Table S9 Genetic distance (F_{ST}) between populations of *L. taliangensis* based on microsatellite data

	PSG	ZUM	ZM	YNH	JHH	XM	GYH	GL	CHJ	LW	BT	SLP	SHK	QLB	WK
PSG															
ZUM	0.236														
ZM	0.087	0.257													
YNH	0.093	0.207	0.100												
JHH	0.033	0.215	0.089	0.056											
XM	0.394	0.364	0.358	0.413	0.357										
GYH	0.153	0.190	0.221	0.134	0.152	0.450									
GL	0.380	0.218	0.358	0.339	0.351	0.369	0.358								
CHJ	0.402	0.275	0.416	0.378	0.373	0.416	0.372	0.212							
LW	0.380	0.258	0.415	0.375	0.355	0.410	0.356	0.278	0.152						
BT	0.571	0.475	0.598	0.562	0.553	0.577	0.536	0.403	0.265	0.337					
SLP	0.496	0.335	0.506	0.475	0.469	0.458	0.466	0.269	0.183	0.200	0.341				
SHK	0.450	0.339	0.472	0.437	0.427	0.465	0.433	0.271	0.131	0.145	0.265	0.194			
QLB	0.389	0.194	0.396	0.352	0.362	0.394	0.362	0.166	0.177	0.227	0.355	0.231	0.234		
WK	0.493	0.336	0.521	0.481	0.477	0.540	0.454	0.270	0.323	0.375	0.511	0.402	0.357	0.210	
YX	0.487	0.275	0.483	0.465	0.464	0.460	0.460	0.178	0.285	0.355	0.492	0.341	0.326	0.186	0.303

Supplementary Table S10 Analysis of molecular variance (AMOVA) for *L. taliangensis* in all populations and two main genetic clusters

Source of variation	*df*	Sum of squares	Variance components	Percentage variation	Fixation indexes
K = 2 (All)					
Among groups	1	478.219	0.974	20.594	$F_{CT} = 0.206$***
Among populations within groups	14	762.095	0.992	20.986	$F_{SC} = 0.264$***
Among individuals within populations	410	1167.275	0.084	1.783	$F_{IS} = 0.031$***
Within individuals	426	1141.000	2.678	56.637	$F_{IT} = 0.434$***
Total	851	3548.588	4.729		
K = 2 (East cluster)					
Among groups	1	132.834	0.494	11.085	$F_{CT} = 0.111$***
Among populations within groups	7	308.907	0.834	18.719	$F_{SC} = 0.211$***
Among individuals within populations	216	686.198	0.048	1.086	$F_{IS} = 0.015$
Within individuals	225	693.000	3.080	69.109	$F_{IT} = 0.309$***
Total	449	1820.938	4.457		
K = 4 (West cluster)					
Among groups	3	291.423	0.900	26.378	$F_{CT} = 0.264$***
Among populations within groups	3	26.591	0.148	4.241	$F_{SC} = 0.059$***
Among individuals within populations	194	484.391	0.134	3.929	$F_{IS} = 0.057$***
Within individuals	201	448.000	2.229	65.352	$F_{IT} = 0.346$***
Total	401	1250.405	3.411		

Note: *df*, degrees of freedom; F_{CT}, fixation index among groups; F_{SC}, fixation index among populations within groups; F_{IS}, fixation index among individuals within populations; F_{IT}, fixation index within individuals

Statistical significance (*P*): *$0.01 < P < 0.05$; **$0.001 < P < 0.01$; ***$P < 0.001$

Supplementary Table S11 Results of bottleneck effect analysis for *L. taliangensis*

Populations	TPM			SMM		
	Hd/He	Sign-test (*P*)	Wilcoxon-test (*P*)	Hd/He	Sign-test (*P*)	Wilcoxon-test (*P*)
XM	6/4	0.213	0.375	7/3	0.083	0.275
ZUM	5/5	0.410	0.625	5/5	0.414	0.922
GYH	6/3	0.152	0.129	7/2	0.039*	0.020*
YNH	5/4	0.355	1.000	5/4	0.330	0.910
JHH	6/3	0.133	0.910	6/3	0.125	0.570
ZM	4/5	0.602	0.734	4/5	0.574	0.734
PSG	4/5	0.591	0.570	4/5	0.612	0.652
GL	5/6	0.483	0.638	5/6	0.476	0.465
SHK	3/7	0.332	0.131	5/5	0.412	0.432
SLP	2/9	0.062	0.206	2/9	0.076	0.206
LW	4/7	0.469	0.765	5/6	0.524	0.577
CHJ	4/7	0.512	0.765	5/6	0.483	0.898
BT	5/5	0.476	0.770	5/5	0.456	0.695
YX	4/7	0.576	0.765	5/6	0.444	0.831
QLB	4/7	0.493	0.413	5/6	0.529	0.700
WK	7/3	0.095	0.322	7/3	0.085	0.232
ALL	8/3	0.037*	0.016*	10/1	0.001***	0.003**
West cluster	8/3	0.035*	0.009**	8/3	0.033*	0.007**
East cluster	7/4	0.115	0.067	9/2	0.007**	0.005**

Note: TPM, two-phase model; SMM, stepwise mutation model; Hd, heterozygosity deficiency; He, heterozygosity excess

Statistical significance (*P*): *$0.01 < P < 0.05$; **$0.001 < P < 0.01$; ***$P < 0.001$

Supplementary Table S12 Results of optimal migration direction between XXL-GG and LS based on microsatellite data

Model	Bezier IML	Ln Bayes factor	Model probability
LS to XXL-GG	-74032.29	-2809.26	0
XXL-GG to LS	-71223.03	0	1
Bi-direction	-137254.53	-66031.50	0

Note: Bezier IML, Bezier log marginal likelihood

Supplementary Table S13 Percentage contribution and permutation importance of bioclimate variables included in ecological niche model (ENM) used for historical distribution analysis

Variable	Description	Percent contribution	Permutation importance
Bio06	Minimum temperature of the coldest month	36.93	17.34
Bio14	Precipitation of the driest month	24.57	34.69
Bio12	Annual precipitation	18.54	20.87
Bio03	Isothermality	17.55	25.34
Bio07	Temperature annual range	2.42	1.75

Supplementary Table S14 Results of multiple matrix regression with randomization (MMRR) analysis for relationship between pairwise genetic distances (F_{ST}) and landscape distances, including geographical resistance distances (IBR) and environmental dissimilarity (IBE)

	Model	R^2	Variable	*P*-value	Coefficient β	t	F	*P*-value (model)
ALL	RD+PC1+PC2	0.163	RD	0.011**	0.405	3.681	7.552	0.011**
			PC1	0.133	0.143	1.557		
			PC2	0.215	-1.679	-1.557		
	RD+PC1	0.146	RD	0.032**	0.300	3.429	9.994	0.011**
			PC1	0.062	0.181	2.064		
	RD	0.115	RD	0.013**	0.339	3.912	15.306	0.013**
	Rejected term							
	PC1+PC2	0.066	PC1	0.015**	0.252	2.808	4.110	0.068
			PC2	0.557	0.075	0.840		
	PC1	0.060	PC1	0.019**	0.245	2.746	7.540	0.019**
West cluster (XXL-GG)	wRD+wPC1+wPC2	0.942	wRD	0.002**	0.982	0.163	91.350	0.002**
			wPC1	0.604	0.037	0.606		
			wPC2	0.627	-0.040	-0.666		
	wRD+wPC1	0.940	wRD	0.002**	0.977	16.590	141.165	0.002**
			wPC1	0.521	0.043	0.733		
	wRD	0.938	wRD	0.001**	0.969	16.995	288.832	0.001**
	Rejected term							

			wPC1	0.577	-0.140	-0.593	0.267	0.819
	wPC1+wPC2	0.029	wPC2	0.793	0.073	0.310		
	wPC1	0.024	wPC1	0.531	-0.154	-0.678	0.459	0.531
			eRD	0.512	0.250	1.182		
	eRD+ePC1+ePC2	0.068	ePC1	0.843	0.054	0.315	0.784	0.786
East cluster (LS)			ePC2	0.984	0.005	0.025		
	eRD+ePC1	0.068	eRD	0.408	0.253	1.507	1.212	0.621
			ePC1	0.834	0.054	0.319		
	eRD	0.066	eRD	0.390	0.256	1.544	2.385	0.390

Note: R^2, coefficient of determination; AICc, Akaike's information criterion and finite corrections; β, regression coefficients; *F*, F-statistics; RD, resistance distance based on the current distribution range prediction raster of *L. taliangensis*; PC1and PC2, two principal components of environmental variables. Alphabet in front of variables represents two genetic clusters respectively.

Statistical significance (*P*): *$0.01 < P < 0.05$; **$0.001 < P < 0.01$; ***$P < 0.001$

Supplementary Table S15 Principal component loading of environmental parameters used for IBE analysis

Environmental parameters	PC1	PC2
Bio01	**0.940**	0.189
Bio02	0.054	-0.904
Bio03	-0.061	**-0.961**
Bio04	0.134	**0.979**
Bio05	0.902	0.38
Bio06	0.901	0.205
Bio07	0.39	0.674
Bio08	0.877	0.413
Bio09	**0.945**	-0.09
Bio10	0.877	0.413
Bio11	**0.945**	-0.09
Bio12	0.543	0.428
Bio13	0.573	-0.164
Bio14	0.34	0.907
Bio15	0.333	-0.902
Bio16	0.665	0.022
Bio17	0.345	**0.912**
Bio18	0.665	0.022
Bio19	0.345	**0.912**
NDVI	0.537	0.521

Note: Data presented in boldface indicates the main environmental variables represented by the principal components

Supplementary Table S16 Percentage contribution and permutation importance of environmental variables included in ENM used for IBR analysis

Variable	Description	Percent contribution	Permutation importance
NDVI	Normalized difference vegetation index	34.33	1.94
Bio14	Precipitation of the driest month	22.81	17.66
Alt	Altitude	20.92	35.14
Bio12	Annual precipitation	9.49	24.44
Bio07	Temperature annual range	3.88	0.53
River	Distance to rivers	3.60	2.53
HII	Human disturbance	2.64	1.72
Bio15	Precipitation seasonality	1.41	3.72
Bio04	Temperature seasonality	0.92	12.31

Supplementary Figures

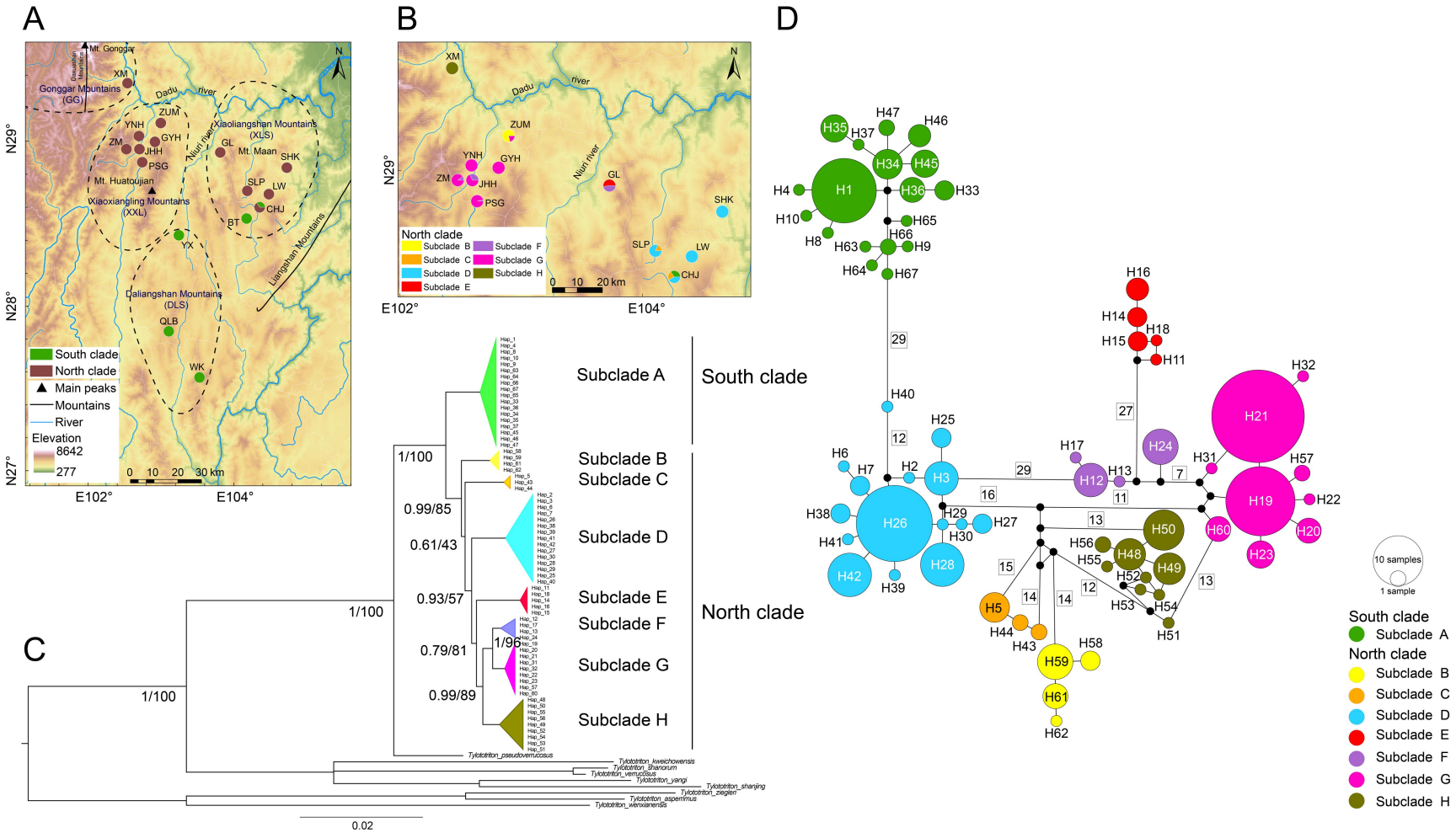

Supplementary Figure S1 Results of the network analysis of the mitochondrial concatenated genes (cyt *b*+*ND2*+*COI*) across *L. taliangensis* distribution range.

(A) Geographic distribution of clades of *L. taliangensis*. Black dashed line represents four main distribution mountains of *L. taliangensis* (i.e., Gonggar (GG), Xiaoxiangling (XXL), Xiaoliangshan (XLS), and Daliangshan mountains (DLS)); (B) Geographic distribution of subclades of *L. taliangensis*. Population codes and number of analyzed sequences are shown in Supplementary Table S1; (C) Maximum-likelihood tree (ML) and Bayesian phylogenetic tree (BI), constructed based on mitochondrial concatenated genes. Numbers on branches indicate Bayesian posterior probabilities/ML bootstrap values; (D) TCS-derived haplotype network of 67 concatenated gene haplotype sequences. Each colored circle represents clade and subclade. Size of circles indicates frequency of each haplotype. Black solid dots represent not detected or extinct ancestral haplotypes. Numbers in boxes represent mutation steps.

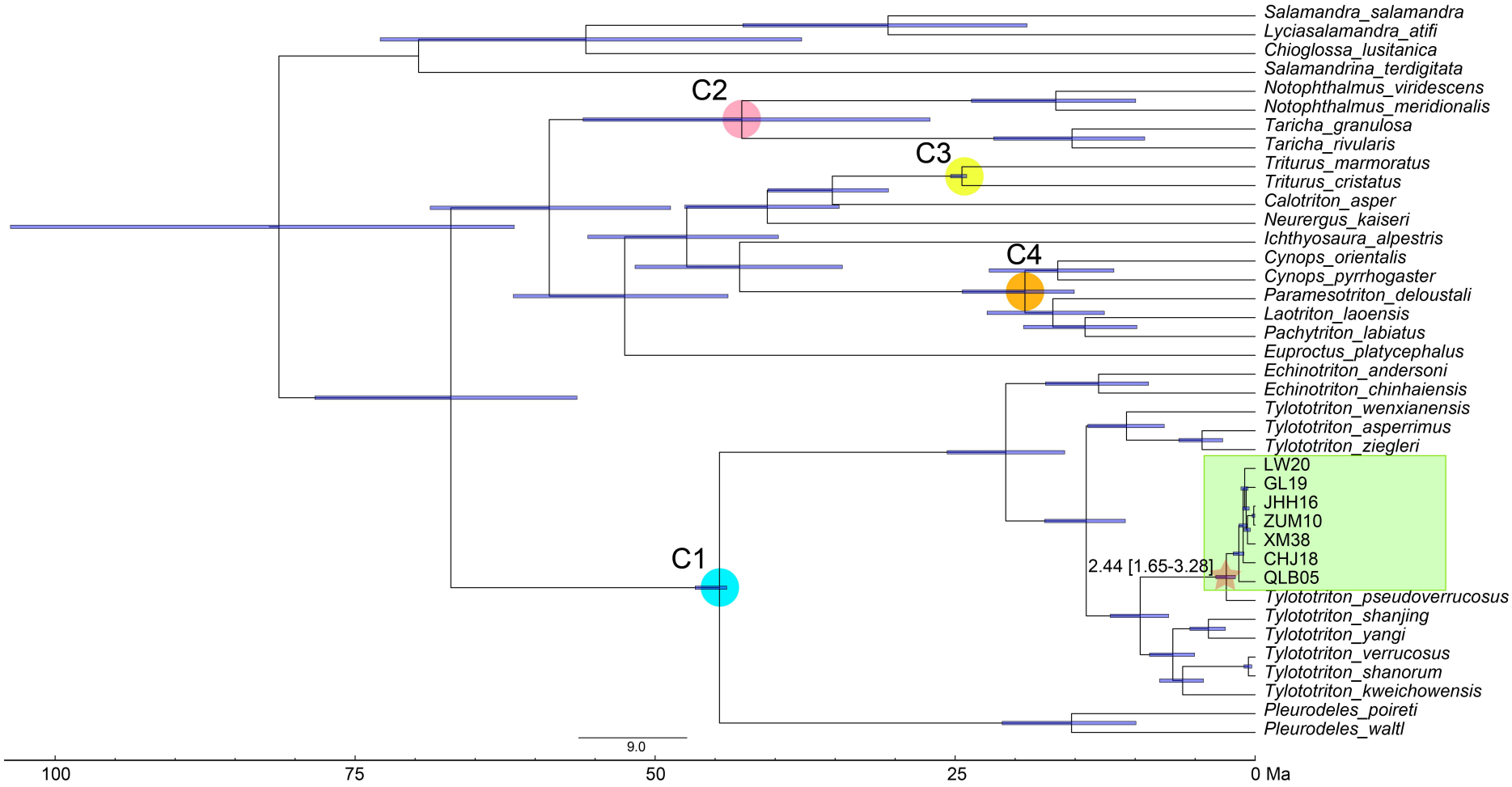
Salamandra_salamandra
Lyciasalamandra_atifi
Chioglossa_lusitanica
Salamandrina_terdigitata
Notophthalmus_viridescens
Notophthalmus_meridionalis
Taricha_granulosa
Taricha_rivularis
Triturus_marmoratus
Triturus_cristatus
Calotriton_asper
Neurergus_kaiseri
Ichthyosaura_alpestris
Cynops_orientalis
Cynops_pyrrhogaster
Paramesotriton_deloustali
Laotriton_laoensis
Pachytriton_labiatus
Euproctus_platycephalus
Echinotriton_andersoni
Echinotriton_chinhaiensis
Tylototriton_wenxianensis
Tylototriton_asperrimus
Tylototriton_ziegleri
LW20
GL19
JHH16
ZUM10
XM38
CHJ18
QLB05
Tylototriton_pseudoverrucosus
Tylototriton_shanjing
Tylototriton_yangi
Tylototriton_verrucosus
Tylototriton_shanorum
Tylototriton_kweichowensis
Pleurodeles_poireti
Pleurodeles_waltl
C1
C2
C3
C4
2.44 [1.65-3.28]
9.0
100
75
50
25
0 Ma

Supplementary Figure S2 Divergence date of most recent common ancestor (MRCA) of *L. taliangensis* and *T. pseudoverrucosus* based on four salamandrid fossil records.

Blue solid circles represent minimum age of first calibration point C1, estimated to be ~44 Ma between *Tylototriton s.l.* and *Pleurodeles*. Pink solid circle represents minimum age of second calibration point C2, estimated to be ~22 Ma between *Taricha* and *Notophthalmus* based on a fossil of *Taricha oligocenica*. Yellow solid circle represents third calibration point C3, which was the common ancestor of *Triturus* and minimum age was ~24 Ma. Orange solid circle represents minimum divergence time of fourth calibration point C4, which was ~15 Ma between *Cynops* and *Paramesotriton*. GenBank numbers and references of all above calibration points are in Supplementary Table S4. Red stars represent date of MRCA (mean and range) of *L. taliangensis* and *T. pseudoverrucosus.* Green box represents analysis range of second step of divergence date, which was used to estimate clade divergence time of *L. taliangensis*.

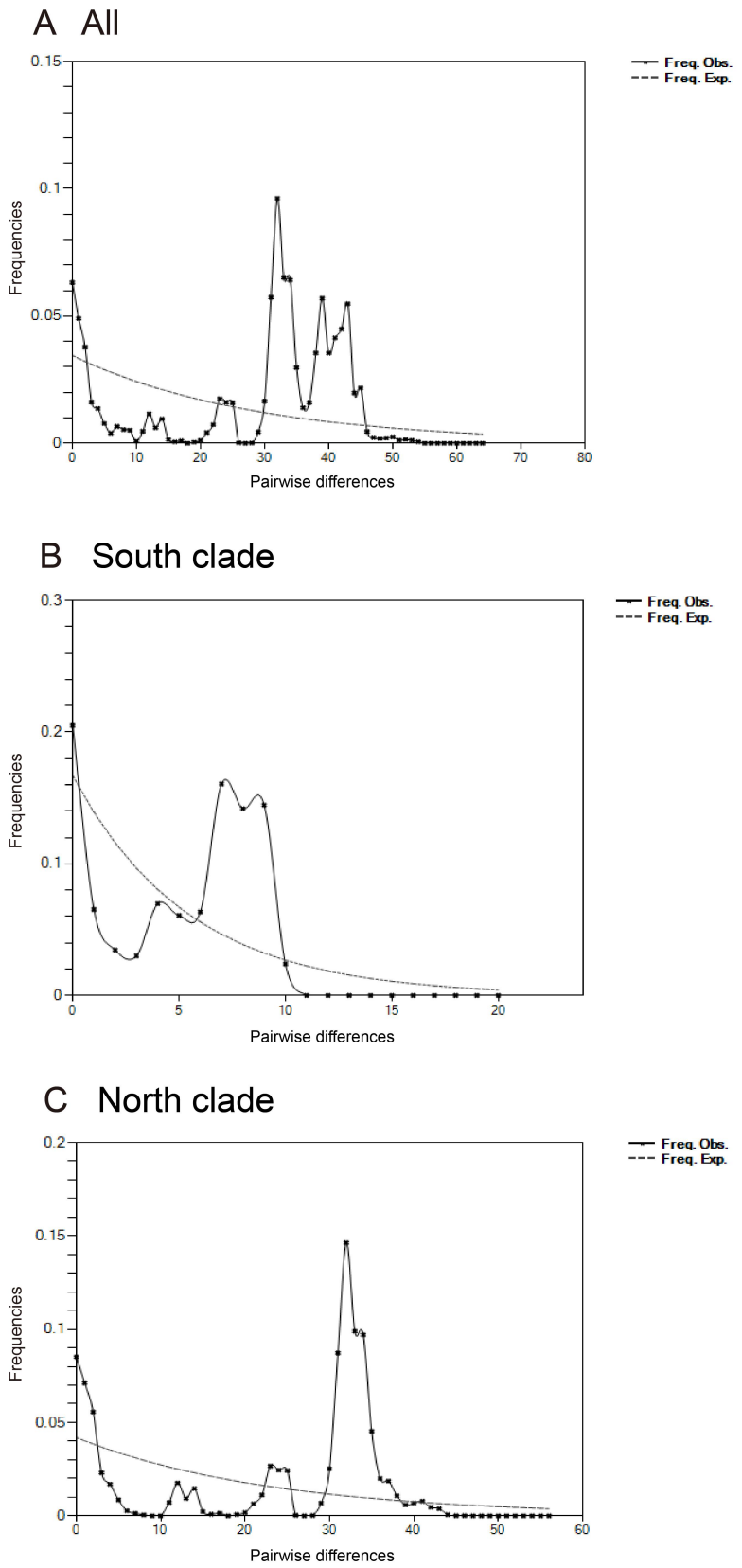

Supplementary Figure S3 Mismatch distribution plot of *L. taliangensis.*

(A) All populations; (B) South clade; (C) North clade.

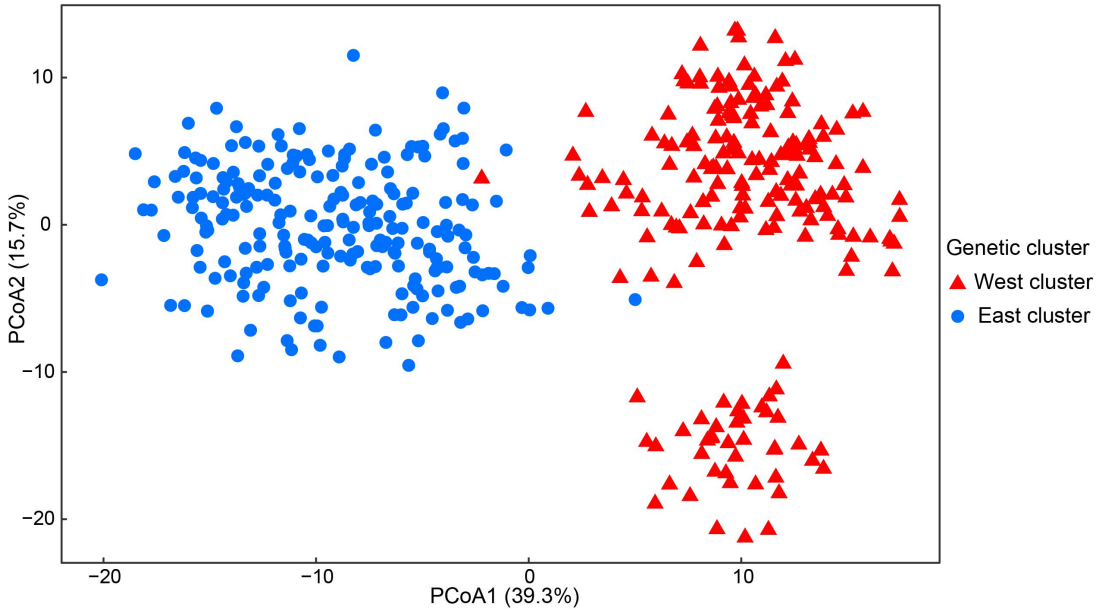

Supplementary Figure S4 Principal coordinate analysis (PCoA) plot of *L. taliangensis* based on microsatellite loci.
West cluster includes populations of XXL-GG mountains, East cluster includes populations of LS mountains (i.e., DLS and XLS).

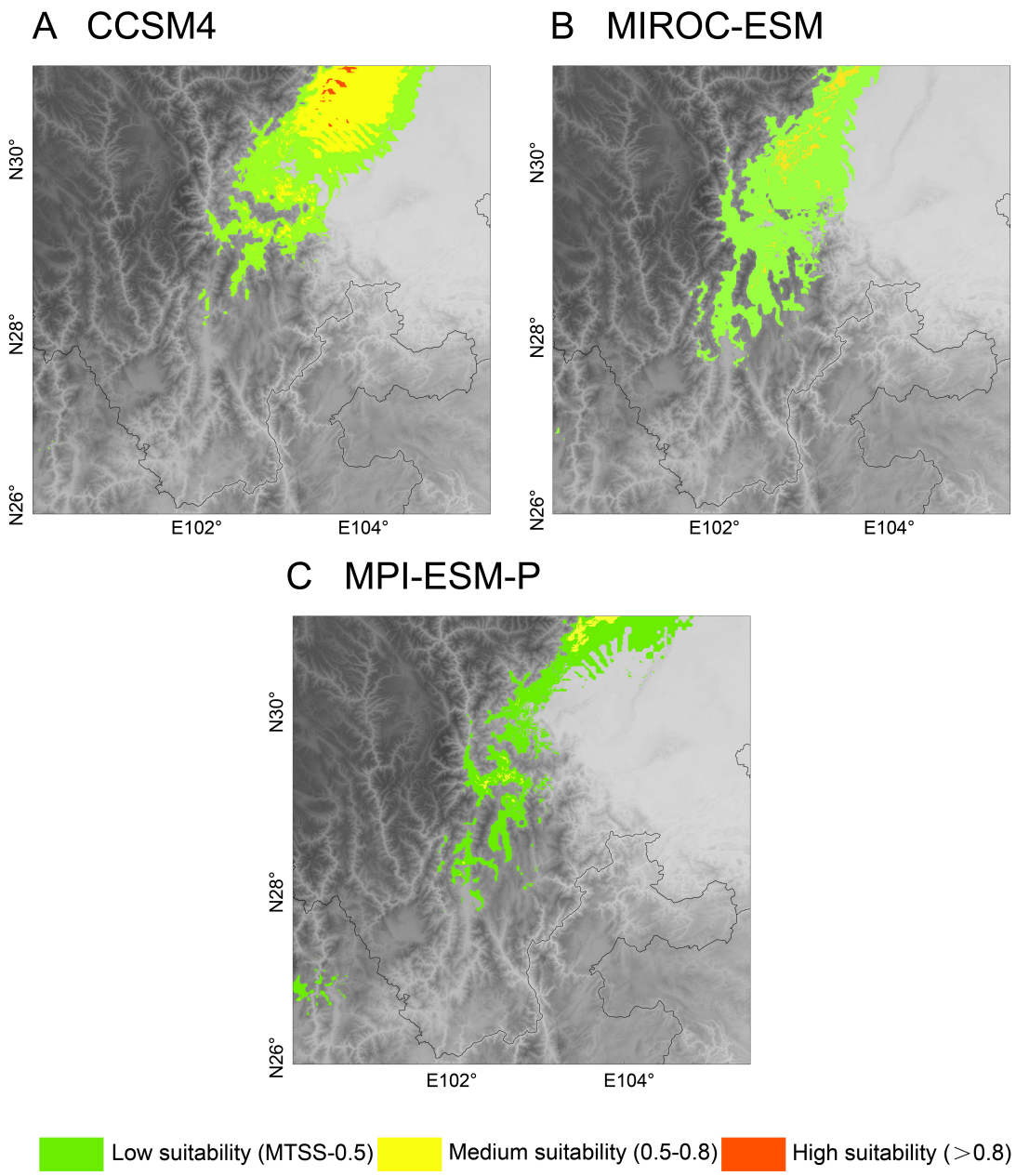

Supplementary Figure S5 Distribution range prediction (averaged from 10 runs) for *L. taliangensis* during LGM based on three different general circulation models (CCSM4, MIROC-ESM, and MPI-ESM-P).
MTSS: maximum training sensitivity plus specificity threshold.

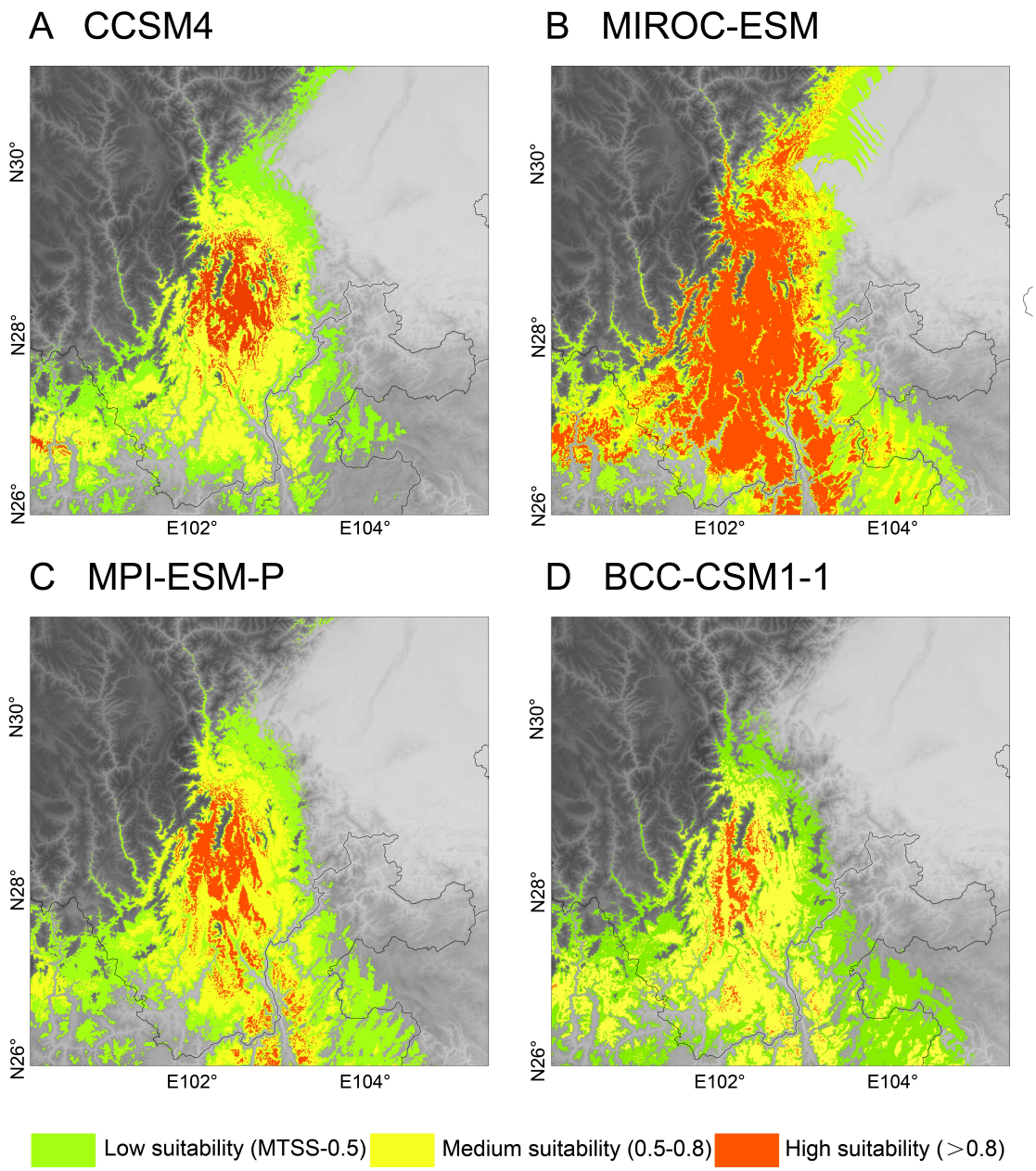

Supplementary Figure S6 Distribution range prediction (averaged from 10 runs) for *L. taliangensis* during MH based on four different general circulation models (CCSM4, MIROC-ESM, MPI-ESM-P, and BCC-CSM1-1).
MTSS: maximum training sensitivity plus specificity threshold.

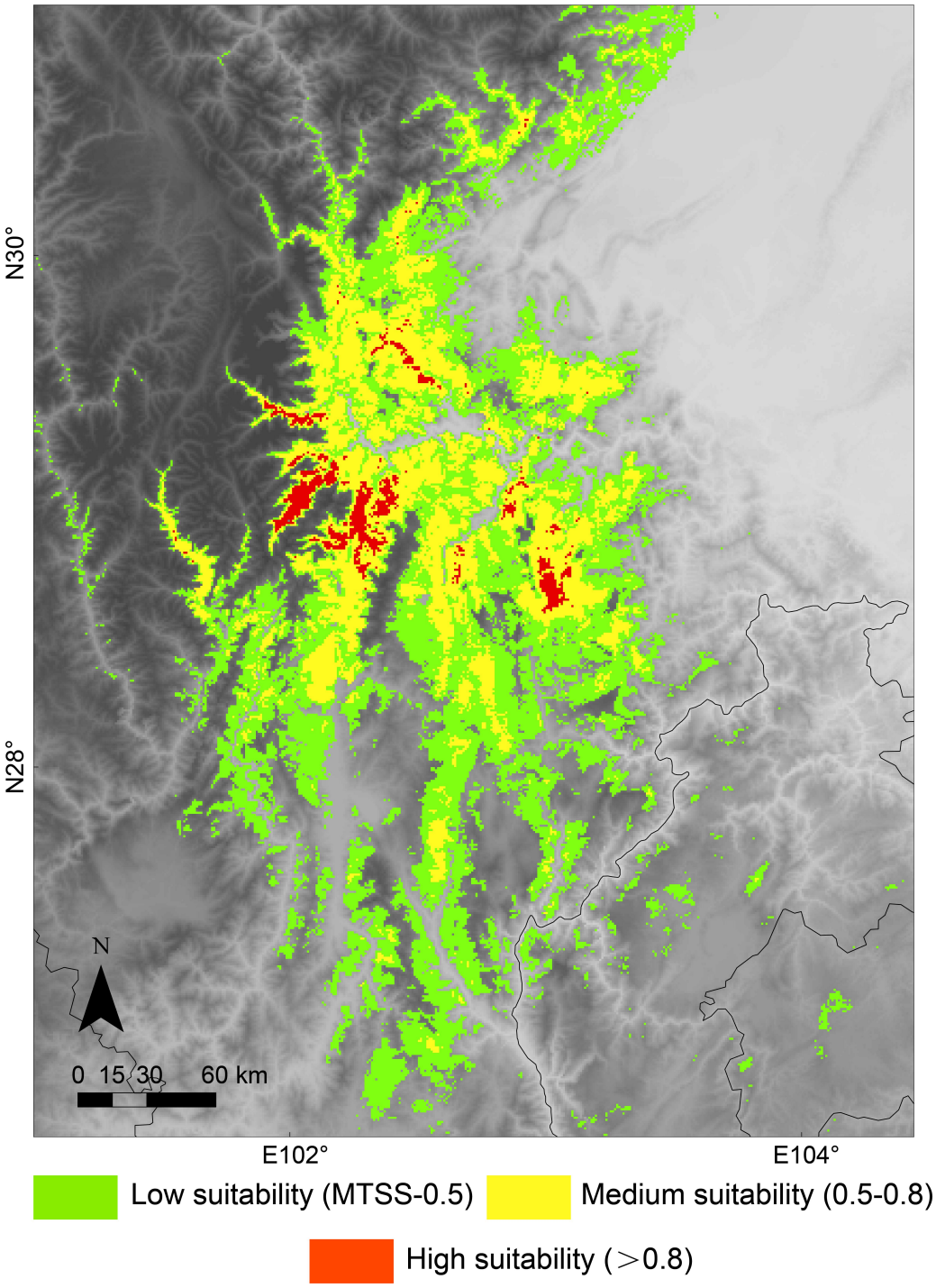

Supplementary Figure S7 Current distribution range prediction raster used for IBR analysis (averaged from 10 runs) of *L. taliangensis* based on bioclimatic, terrain, and human variables.

MTSS: maximum training sensitivity plus specificity threshold.

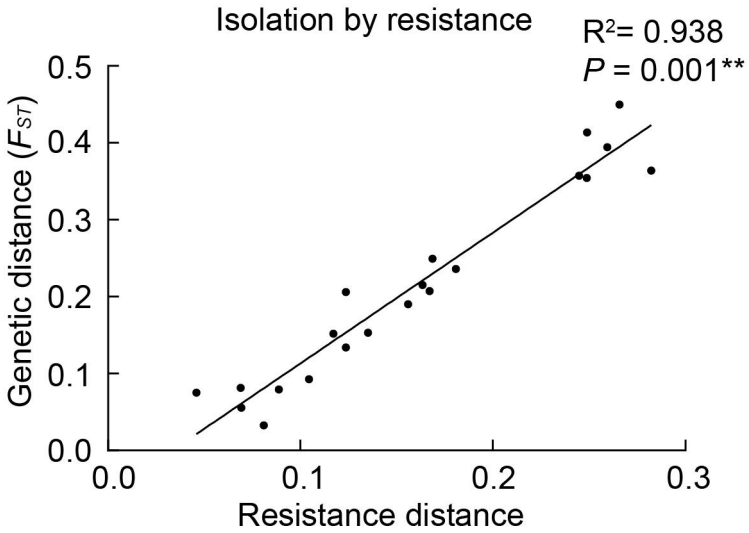

Supplementary Figure S8 Correlations between genetic distance (F_{ST}) and resistance distance (IBR) of West cluster (XXL-GG).

Supplementary References

Beerli P, Palczewski M. 2010. Unified framework to evaluate panmixia and migration direction among multiple sampling locations. *Genetics*, **185**(1): 313–326.

Böhme M. 2003. The Miocene climatic optimum: evidence from ectothermic vertebrates of Central Europe. *Palaeogeography*, *Palaeoclimatology*, *Palaeoecology*, **195**(3–4): 389–401.

Chen DQ, Dong ZJ, Fang M, Fu JJ, Jia XY, Jiang BJ, et al. 2019. Microsatellite records for volume 11, issue 1. *Conservation Genetics Resources*, **11**(1): 109–112.

Drummond AJ, Rambaut A. 2007. BEAST: Bayesian evolutionary analysis by sampling trees. *BMC Evolutionary Biology*, **7**(1): 214.

Emel SL, Wang SC, Metz RP, Spigler RB. 2021. Type and intensity of surrounding human land use, not local environment, shape genetic structure of a native grassland plant. *Molecular Ecology*, **30**(3): 639–655.

Estes R. 1981. Gymnophiona, Caudata. Handbuch der Paläoherpetologie–Encyclopedia of Paleoherpetology Part 2. New York: Gustav Fischer Verlag, 1–115.

Herre W. 1935. Die Schwanzlurche der mitteleocänen (oberlutetischen) Braunkohle des Geiseltales u. die Phylogenie der Urodelen unter Einschluß der fossilen Formen. *Zoologica*, **33**(87): 1–85.

Lanfear R, Frandsen PB, Wright AM, Senfeld T, Calcott B. 2017. PartitionFinder 2: new methods for selecting partitioned models of evolution for molecular and morphological phylogenetic analyses. *Molecular Biology and Evolution*, **34**(3): 772–773.

McRae B, Shah V, Edelman A. 2016. Circuitscape: modeling landscape connectivity to promote conservation and human health. Fort Collins: The Nature Conservancy.

McRae BH. 2006. Isolation by resistance. *Evolution*, **60**(8): 1551–1561.

McRae BH, Dickson BG, Keitt TH, Shah VB. 2008. Using circuit theory to model connectivity in ecology, evolution, and conservation. *Ecology*, **89**(10): 2712–2724.

Milner AR. 2000. Mesozoic and tertiary Caudata and Albanerpetontidae. *In*: Heatwole H, Carroll RL. Amphibian Biology. Chipping Norton: Surrey Beatty & Sons, 1412–1444.

Moritz C, Schneider CJ, Wake DB. 1992. Evolutionary relationships within the *Ensatina eschscholtzii* complex confirm the ring species interpretation. *Systematic Biology*, **41**(3): 273–291.

Myers EA, Xue AT, Gehara M, Cox CL, Davis Rabosky AR, Lemos-Espinal J, et al. 2019. Environmental heterogeneity and not vicariant biogeographic barriers generate community-wide population structure in desert-adapted snakes. *Molecular Ecology*, **28**(20): 4535–4548.

Rambaut A, Drummond AJ, Xie D, Baele G, Suchard MA. 2018. Posterior summarization in Bayesian phylogenetics using Tracer 1.7. *Systematic Biology*, **67**(5): 901–904.

Shu XX, 2020. Conservation Genetics and Habitat Selection of Taliang Knobby Newt (*Liangshantriton Taliangensis*). Sichuan University, Chengdu. (in Chinese)

Vasconcellos MM, Colli GR, Weber JN, Ortiz EM, Rodrigues MT, Cannatella DC. 2019. Isolation by instability: historical climate change shapes population structure and genomic divergence of treefrogs in the Neotropical Cerrado savanna. *Molecular Ecology*, **28**(7): 1748–1764.

Wang B, Jiang JP, Xie F, Chen XH, Dubois A, Liang G, et al. 2009. Molecular phylogeny and genetic identification of populations of two species of *Feirana* frogs (Amphibia: Anura, Ranidae, Dicroglossinae, Paini) endemic to China. *Zoological Science*, **26**(7): 500–509.

Wang IJ. 2013. Examining the full effects of landscape heterogeneity on spatial genetic variation: a multiple matrix regression approach for quantifying geographic and ecological isolation. *Evolution*,

67(12): 3403–3411.
Wang IJ, Bradburd GS. 2014. Isolation by environment. *Molecular Ecology*, **23**(23): 5649 – 5662.
Warren DL, Glor RE, Turelli M. 2010. ENMTools: a toolbox for comparative studies of environmental niche models. *Ecography*, **33**(3): 607–611.
Wright S. 1943. Isolation by distance. *Genetics*, **28**(2): 114–138.